SOUTH POLE - AITKEN BASIN AS A PROBE TO THE LUNAR INTERIOR. D. P. Moriarty III[1] and C. M. Pieters[1], [1]Department of Earth, Environmental, and Planetary Sciences, Brown University, Providence, RI 02912 [Daniel_Moriarty@Brown.edu]

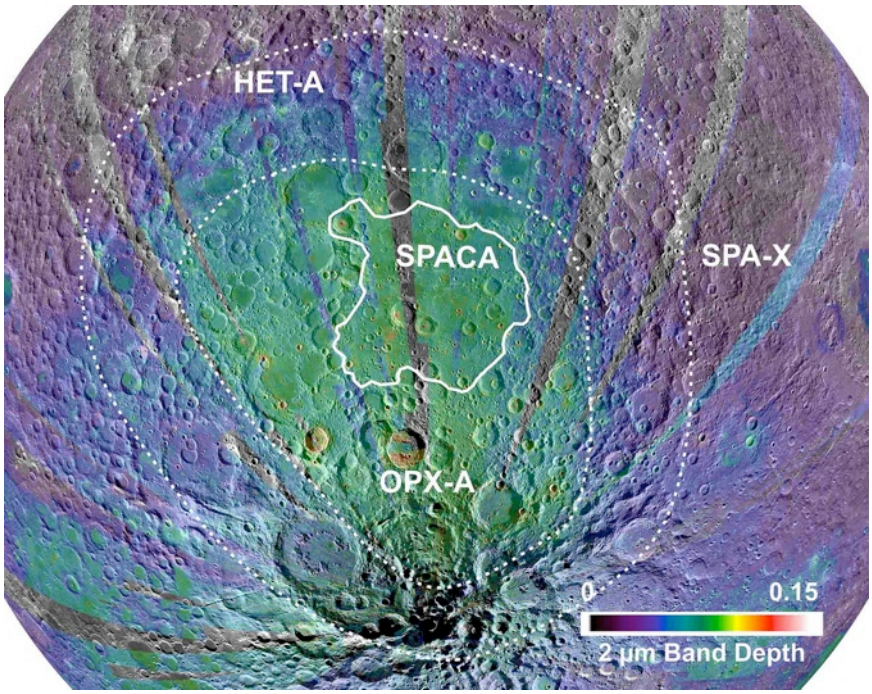

Fig. 1: M^3-derived band depth superimposed on a WAC mosaic. The boundaries of SPACA, OPX-A, HET-A, and SPA-X are given.

Introduction: The ~2200 km South Pole - Aitken Basin (SPA) is largest well-preserved impact basin on the Moon[1-3]. Materials excavated by the SPA impact are thought to be some of the deepest lunar materials available for study, either through remote sensing or future sample return. In this analysis, we combine M^3[4] spectra with LOLA[5] topography and LROC[6] imagery to investigate the composition and distribution of materials excavated in the SPA-forming impact. Building on the general SPA properties described in [7], we define 4 distinct compositional regions related to basin formation and evolution.

Approach: The SPA interior exhibits a pyroxene-dominated composition[8]. Therefore, compositional variations within SPA materials can be characterized using the NIR pyroxene absorption bands around 1 µm and 2 µm [9-11]. Variations in pyroxene abundance are captured by band depth measurements. Variations in pyroxene composition are captured by band center measurements. Generally, Mg-rich orthopyroxenes (OPX) exhibit the shortest-wavelength band centers, while Ca,Fe-rich clinopyroxenes (CPX) exhibit the longest -wavelength band centers[9-11].

A map of 2 µm absorption band depth is presented in Fig. 1, highlighting variations in mafic abundance across SPA. A map of 2 µm absorption band center for areas with significant mafic content is presented in Fig. 2, projected onto a topographic basemap. Compositional diversity and stratigraphy in complex craters and basins across SPA are represented schematically, and mare basalts have been masked.

The "central SPA Compositional Anomaly" (SPACA) [12] region indicated in Fig. 1 is dominated by materials with relatively strong, long-wavelength absorption bands, indicating an average pyroxene composition with significant CPX. As noted in [12,13], these materials probably do not represent pristine products of the SPA-forming impact. Instead, they represent either impact melt or early volcanic deposits[12].

Immediately outside of the SPACA, average band center values shift to much shorter wavelengths (consistent with Mg-rich pyroxenes), while band depth values remain uniformly elevated. This "OPX Annulus" (OPX-A) appears relatively homogeneous in composition over a wide range of exposures, from small surficial craters (<1 km) to the walls, peaks, rings, floors, and ejecta of larger craters such as Lyman (84 km) and Antoniadi (143 km), as well as the southern portion of Apollo Basin (538 km).

Exterior to the OPX-A, localized areas exhibiting mafic signatures are heterogeneously mixed with more feldspathic areas. The dominant mafic component in this "Heterogeneous Annulus" (HET-A) exhibits short wavelength absorption bands similar to materials in the OPX-A. A gradient in the prevalence of mafic exposures as well as the overall mafic content of soils is observed with distance from OPX-A.

The outer boundary of the HET-A roughly corresponds to the topographic rim of SPA. Exterior to this (SPA Exterior / SPA-X), most materials exhibits featureless spectra indicating a negligible mafic component. Of course, local areas such as Australe to the southwest exhibit significant mare basalt emplacements.

Discussion: Outside of the SPACA (which exhibits CPX-bearing materials not representative of pristine SPA ejecta [12]), the OPX-A represents an expanse of relatively homogeneous material dominated by Mg-rich pyroxenes. The uniform presence of these materials in the walls and peaks of several large craters and basins indicates that this component is at least several tens of

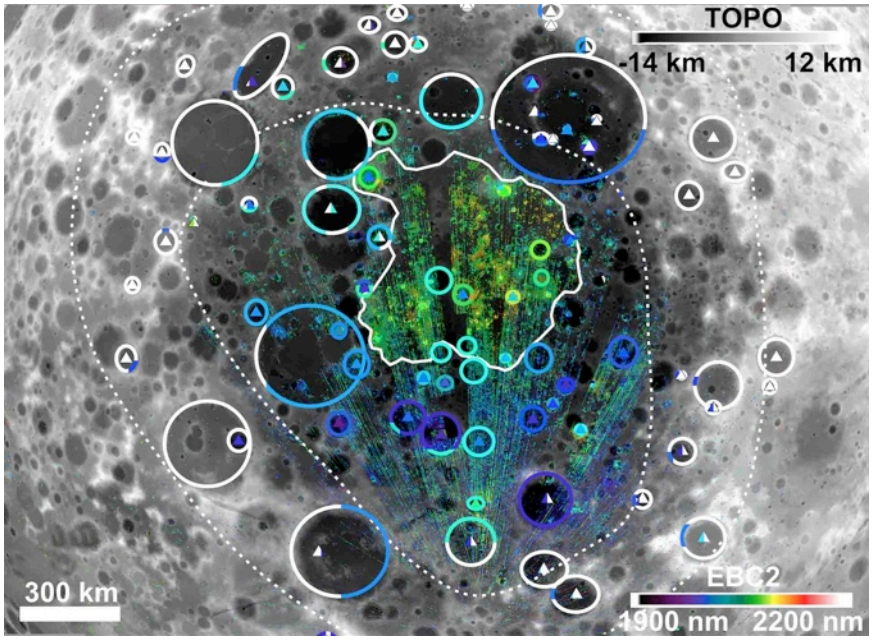

Fig. 2: M^3-derived 2 µm absorption band center (EBC2) overlaid on LOLA topography. Superposed symbols for prominent complex craters highlight the local compositional diversity and stratigraphy. Symbol colors correspond to the EBC2 map, with white indicating the presence of feldspathic materials. Ellipses correspond to crater rims and walls, while triangles correspond to central peaks. The approximate extents of SPACA (solid), OPX-A, HET-A, and SPA-X (dashed) are given.

km thick, and there is no evidence that this layer terminates anywhere in the near-surface. Due to the large lateral extent and vertical thickness of OPX-A, we conclude that this region represents pristine excavated materials from a very thick, relatively homogeneous layer of the pre-impact region.

Impact models suggest that the transient cavity associated with the SPA impact was likely between ~500 and ~1150 km[14]. If the maximum excavation depth is ~10% of the transient cavity diameter[15], the SPA-forming impact excavated material from up to ~50-100 km beneath the pre-impact surface. Since the lunar feldspathic crust is estimated to be ~40 km thick [16], the impact should have excavated through the crust. Therefore, sub-crustal materials would be present in the walls and floor of the transient cavity. Although the transient cavity is by definition "transient," remnant portions of the structure likely comprise portions of the SPA interior. These materials probably also include significant volumes of impact melt and breccia bearing the bulk composition of the excavated material. OPX-A is interpreted to represent remnant portions of a collapsed transient cavity which exposed material from a thick, uniform sub-crustal layer.

The HET-A provides further evidence of sub-crustal components. Impact models suggest that the deepest-seated ejecta in an impact typically are typically emplaced close to the transient cavity rim[14]. For SPA, most of the proximal ejecta is deposited within a region that then slumps and collapses inward during the modification stage[14]. Therefore, the deepest excavated material largely remains within the current SPA rim[14]. This proximal ejecta initially lands exterior to the transient cavity on the feldspathic highlands. These crustal materials would have undergone large-scale mixing with SPA ejecta during ejecta deposition and large-scale faulting and collapse of the transient cavity, producing the HET-A.

Conclusions: Combining compositional assessment with geophysical models, there is evidence for large-scale exposure of subcrustal materials in two distinct SPA regions. The laterally extensive, vertically thick OPX-A, which exhibits a homogeneous composition dominated by Mg-rich pyroxenes may correspond to a remnant portion of the SPA transient cavity that excavated through the ~40 km feldspathic crust. Exterior to this region, the HET-A, which contains discontinuous areas of similar pyroxene-rich material, is likely host to ejected sub-crustal materials mixed with feldspathic crust during ejecta emplacement and basin modification. Since the Mg-rich pyroxenes are predicted to originate from beneath the crust, it is reasonable to suggest that they represent upper mantle compositions. The SPACA in central SPA has been affected by impact melt and/or volcanic flooding, and is therefore not likely to be representative of pristine compositions.

The compositional character of SPA is becoming better understood, and the relationships between different components are well defined. What is less clear is whether the distinctive OPX-A and HET-A represent (a) upper mantle as predicted by cratering models, or (b) lower crust enriched in Mg-suite materials [17].

Acknowledgements: This analysis is supported through NASA LASER (NNX12AI96G) and SSERVI (NNA14AB01A).

References: [1]Stuart-Alexander, D. E. 1978, *USGS.* [2]Spudis, P. D. et al. 1994, *Sci., 266:*1848-1851. [3]Garrick-Bethell, I. and M. T. Zuber 2009, *Icar., 204:*399-408. [4]Pieters, C. M. et al. 2009, *Curr. Sci. 96:*4:500-505. [5]Smith, D. E. et al. 2010, *Geo. Res. Let., 37:* L18204. [6]Robinson, M. S. et al. 2010, *Spa. Sci. Rev., 150:*1-4:81-124. [7]Jolliff, B. L. et al. 2000, *J. Geo. Res. 105:*4197-4216. [8] Pieters, C. M. et al. 2001, *J. Geo. Res. 106:*28001-28022. [9]Moriarty, D. M. and C. M. Pieters 2016, *Met. and Plan. Sci.,* in press. [10] Klima, R. L. et al. 2007, *Met. and Plan. Sci, 42:*2:228-251. [11]Klima, R. L. et al. 2011, *Met. and Plan. Sci., 46:*3:379-395. [12]Moriarty, D. M. and C. M. Pieters 2016, *LPSC 47.* [13]Ohtake, M. et al. 2014, *Geo. Res. Let. 41:*2738-2745. [14]Potter, R. W. K. et al. 2012, *Icar. 220:* 730-743. [15]Melosh, H. J. 1989, *Imp. Crat.,* Ox. Press. [16] Wieczorek, M. A. et al. 2013, *Sci. 339:*6120:671-675. [17]Shearer, C. K. et al. 2015, *Am. Min. 100:*294-325.